

De-Confinement and the Clustering of Color Sources

BRIJESH K SRIVASTAVA^{*}

Department of Physics & Astronomy, Purdue University West Lafayette, Indiana, USA

(Received on 26 April 2014; Accepted on 9 September 2014)

A brief review of the color string percolation model (CSPM) is presented. The clustering of color sources provides a framework of the partonic interactions in the initial stage of the collisions. The CSPM has described several observables in agreement with the experimental results e.g. multiplicity, elliptic flow at RHIC and LHC energies. The thermodynamical quantities temperature and the Equation Of State (EOS) are obtained in agreement with the Lattice Quantum Chromo Dynamics (LQCD) calculations. The shear viscosity to entropy density ratio (η/s) is obtained at RHIC and LHC energies. It is also observed that the inverse of η/s is equivalent to trace anomaly $\Delta = (\varepsilon - 3P)/T^4$ in excellent agreement with the recent LQCD calculations.

Key Words : Relativistic Heavy-Ion Collisions; Percolation; QGP; EOS

Introduction

One of the main goal of the study of relativistic heavy ion collisions is to study the deconfined matter, known as Quark-Gluon Plasma (QGP), which is expected to form at large densities. It has been suggested that the transition from hadronic to QGP state can be treated by percolation theory (Celik *et al.*, 1980). The formulation of percolation problem is concerned with elementary geometrical objects placed on a random d-dimensional lattice. Several object can form a cluster of communication. At certain density of the objects a spanning cluster appears, which marks the percolation phase transition. This is defined by the dimensionless percolation density parameter ξ (Isichenko, 1992). In nuclear collisions there is indeed, as a function of parton density, a sudden onset of large scale color connection. Percolation would correspond to the onset of color deconfinement and it may be a prerequisite for subsequent formation of the QGP. Fig. 1 shows the parton distribution in the transverse plane of a overlapping region of low and high density partons.

^{*} Author for Correspondence : E-mail: brijesh@purdue.edu

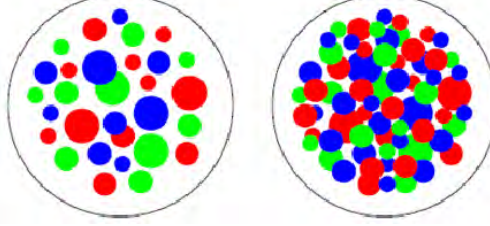


Fig. 1: Partonic cluster structure in the transverse collision plane at low (A) and (B) high parton density (Satz, 2012)

In this talk we present some of the results from the Color String Percolation Model (CSPM) e.g. for the multiplicity and elliptic flow in A+A collisions. Results are also presented for the temperature, equation of state and the transport coefficient.

Clustering of Color Sources

Multi-particle production at high energies can be described at an effective level in terms of color strings stretched between the projectile and target. Color strings may be viewed as small discs in the transverse space filled with the color field created by colliding partons. These strings act as color sources of emitted particles through the creation of $q\bar{q}$ pairs as they split. Subsequent hadronization produces the observed hadrons. With growing energy and size of the colliding nuclei the number of strings grow and start to overlap to form clusters, very much similar to the disks in the 2D percolation theory (Braun and Pajares, 2000, Braun *et al.*, 2002). At a certain critical density a macroscopic cluster appears that marks the percolation phase transition. This is termed as Color String percolation Model (CSPM) (Braun and Pajares 2000; Braun *et al.*, 2002). The string density ξ is defined as $N_s S_1 / S_n$ where N_s is the number of strings, S_1 the transverse area of a single string, $S_1 = \pi r_0^2$ and S_n the overlap area of the collision, which depends on the impact parameter. The interaction between strings occurs when they overlap and the general result, due to the SU(3) random summation of charges, is a reduction in the multiplicity and an increase in the string tension or an increase in the average transverse momentum squared, $\langle p_t^2 \rangle$.

CSPM is a saturation model similar to the Color Glass Condensate (CGC) (McLerran and Venugopalan, 1994; Dias and Pajares, 2011). In CGC the saturation phenomena results from the overcrowding in impact parameter of low x partons. The role of the saturation momentum Q_s^2 is given by $\sqrt{\xi}$.

Knowing the color charge \vec{Q}_n one can obtain the multiplicity μ and the mean transverse momentum squared $\langle p_t^2 \rangle$ of the particles produced by a cluster of n strings (Braun *et al.*, 2002)

$$\mu_n = \sqrt{\frac{n S_n}{S_1}} \mu_0; \quad \langle p_t^2 \rangle = \sqrt{\frac{n S_1}{S_n}} \langle p_t^2 \rangle_1 \quad (1)$$

where μ_0 and $\langle p_t^2 \rangle_1$ are the mean multiplicity and average transverse momentum squared of particles produced from a single string with a transverse area $S_1 = \pi r_0^2$. In the thermodynamic limit, one obtains an

analytic expression (Braun and Pajares, 2000, Braun *et al.*, 2002).

$$\left\langle \frac{nS_1}{S_n} \right\rangle = \frac{\xi}{1 - e^{-\xi}} \equiv \frac{1}{F(\xi)^2} \quad (2)$$

where $F(\xi)$ is the color suppression factor. In the above expression the factor $1 - e^{-\xi}$ is the fraction of the total area of the collision covered by strings. Close to the critical percolation point the area covered by strings is $\sim 2/3$. $\xi = \frac{N_S S_1}{S_N}$ is the percolation density parameter assumed to be finite when both the number of strings N_S and total interaction area S_N are large.

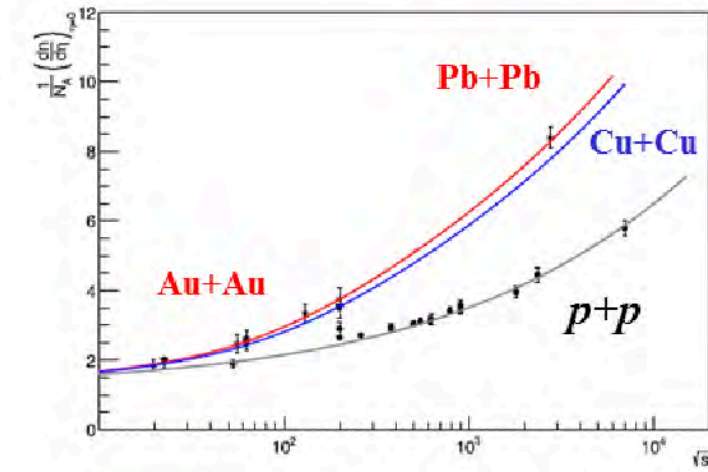


Fig. 2: Comparison of the evolution of the mid-rapidity multiplicity with energy from the CSPM and data for pp and A+A collisions. Lines are from the model for pp (grey), Cu+Cu(blue) and red lines for Au+Au/Pb+Pb (Bautista *et al.*, 2012)

Multiplicity in pp and A+A Collisions

Measurements of particle multiplicities constrain the early time properties of colliding systems. In A+A case, these measurements are an essential ingredient for the estimation of the initial energy and entropy densities. The system will eventually thermalize to form the QGP. The charged particle multiplicity in A+A collisions at mid-rapidity is given by (Bautista *et al.*, 2012).

$$\frac{1}{N_A} \frac{dn^{AA}}{dy} = \frac{dn^{pp}}{dy} \left(1 + \frac{F(\xi)_{AA}}{F(\xi)_{pp}} (N_A^{\alpha(\sqrt{s})} - 1) \right) \quad (3)$$

where $F(\xi)_{AA}$ and $F(\xi)_{pp}$ are the color suppression factor for A+A and p-p collisions. N_A is the average number of participating nucleons. $\alpha(\sqrt{s})$ is a function of center of mass energy(s) and in high energy limit it approaches 1/3 (Bautista *et al.*, 2012). Fig. 2 shows a comparison of the evolution of the mid rapidity multiplicity with energy given by Eq.(3) with data for pp and A+A collisions. It is observed that the power law dependence of the multiplicity on the collision energy is the same in pp and AA collisions. The faster

growth in the AA case is due to the opening of energy-momentum constraints which control string creation, and thus the multiplicity, at low energy.

Elliptic Flow v_2

The cluster formed by the strings has generally an asymmetric form in the transverse plane and acquires dimensions comparable to the nuclear overlap. This azimuthal asymmetry is at the origin of the elliptic flow in CSPM. The partons emitted at some point inside the cluster have to pass through the strong color field before appearing on the surface. The energy loss by the parton is proportional to the length and therefore the p_t of a particle will depend on the direction of the emission (Bautista *et al.*, 2011). The percolation density parameter ξ will be azimuthal angle dependent $\xi_\phi = \xi(R/R_\phi)^2$. The v_2 expressed in terms of ξ is given by (Bautista *et al.*, 2011; Braun and Pajares, 2011).

$$v_2 = \frac{2}{\pi} \int_0^\pi d\phi \cos(2\phi) \left(\frac{R_\phi}{R} \right) \left(\frac{e^{-\xi} - F(\xi)^2}{2F(\xi)^3} \right) \frac{R}{R-1} \quad (4)$$

where R is the radius of the projected circle and azimuthal dependence of R is given by R_ϕ . The transverse momentum dependence of v_2 computed using Eq.(4) for Pb+Pb at $\sqrt{s_{NN}}=2.76$ TeV and Au+Au at $\sqrt{s_{NN}}=200$ GeV is shown in Fig.3. The results are in good agreement with the ALICE and STAR results for 10 – 20% centrality.

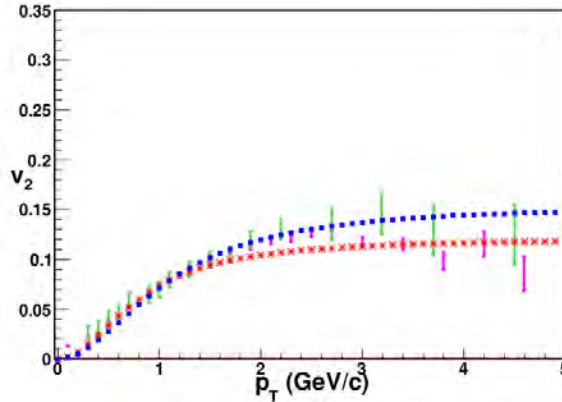


Fig. 3: Elliptic flow v_2 comparison with data and CSPM. The error bars in red and green are the results from Pb+Pb at $\sqrt{s_{NN}}=2.76$ TeV and Au+Au at $\sqrt{s_{NN}}=200$ GeV. The CSPM results are shown as dotted blue and red lines (Braun and Pajares, 2011)

Experimental Determination of the Color Suppression Factor $F(\xi)$

The suppression factor is determined by comparing the pp and A+A transverse momentum spectra. To evaluate the initial value of $F(\xi)$ from data for Au+Au collisions, a parameterization of pp events at 200

GeV is used to compute the p_t distribution $dN_c/dp_t^2 = a/(p_0 + p_t)^\alpha$ (Scharenberg *et al.*, 2011). where a is the normalization factor, p_0 and α are parameters used to fit the data. This parameterization also can be used for nucleus-nucleus collisions to take into account the interactions of the strings (Braun *et al.*, 2002)

$$dN_c/dp_t^2 = \frac{a'}{(p_0 \sqrt{F(\xi_{pp})/F(\xi_{AA})} + p_t)^\alpha} \quad (5)$$

with $F(\xi_{pp}) \sim 1$. Fig. 4 shows a plot of $F(\xi)$ as a function of charged particle multiplicity per unit transverse area $\frac{dN_c}{d\eta}/S_N$ for Au+Au collisions at 200 GeV for various centralities for the STAR data (Scharenberg *et al.*, 2011; Abelev *et al.*, 2009). $F(\xi)$ decreases in going from peripheral to central collisions. The ξ value is obtained using Eq.(5), which increases with the increase in centrality. The fit to the Au+Au points has the functional form $F(\xi) = \exp[-0.165 - 0.094 \frac{dN_c}{d\eta}/S_N]$. Recently, the ALICE experiment at LHC published the charged-particle multiplicity density data as a function of centrality in Pb+Pb collisions at $\sqrt{s_{NN}} = 2.76$ TeV (Aamodt *et al.*, 2011). The ALICE data points are shown in Fig. 4.

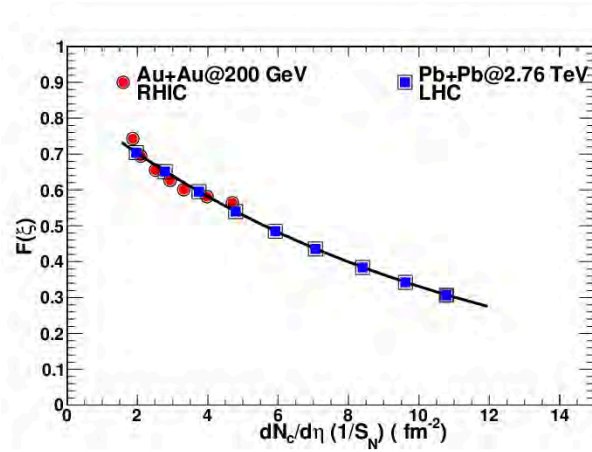


Fig. 4: Color suppression factor $F(\xi)$ as a function of $\frac{dN_c}{d\eta}/S_N (fm^{-2})$. The solid red circles are for Au+Au collisions at 200 GeV(STAR data). The error is smaller than the size of the symbol. The line is fit to the STAR data. The solid blue squares are for Pb+Pb at 2.76 TeV

Energy Density ε

The QGP according to CSPM is born in local thermal equilibrium because the temperature is determined at the string level. After the initial temperature $T > T_c$ the CSPM perfect fluid may expand according to Bjorken boost invariant 1D hydrodynamics (Bjorken, 1983)

$$\varepsilon = \frac{3}{2} \frac{\frac{dN_c}{dy} \langle m_t \rangle}{S_n \tau_{pro}} \quad (6)$$

where ε is the energy density, S_n nuclear overlap area, and τ_{pro} the proper time. Above the critical temperature only massless particles are present in CSPM. To evaluate ε we use the charged pion multiplicity dN_c/dy at midrapidity and S_n values from STAR for 0-10% central Au-Au collisions with $\sqrt{s_{NN}} = 200$ GeV (Scharenbeg *et al.*, 2011). The factor 3/2 in Eq.(6) accounts for the neutral pions. The average transverse mass $\langle m_t \rangle$ is given by $\langle m_t \rangle = \sqrt{\langle p_t \rangle^2 + m_0^2}$, where $\langle p_t \rangle$ is the transverse momentum of pion and m_0 being the mass of pion $\tau_{pro} = \frac{2.405\hbar}{\langle m_t \rangle}$.

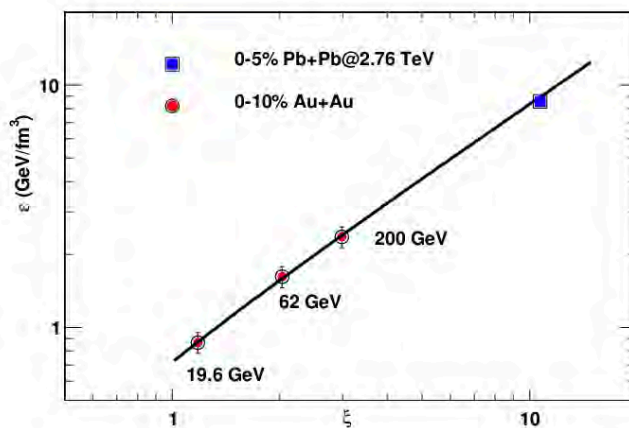


Fig. 5: Energy density ε as a function of the percolation density parameter ξ . The extrapolated value for LHC energy is shown as blue square (Dias *et al.*, 2012)

In CSPM the total transverse energy is proportional to ξ . From the measured value of ξ and ε , as shown in Fig.5, it is found that ε is proportional to ξ for the range $1.2 < \xi < 2.88$, $\varepsilon = 0.788 \xi \text{ GeV}/fm^3$ (Dias *et al.*, 2012). The extrapolated value of ε for central Pb+Pb collision at 2.76 TeV is $8.32 \text{ GeV}/fm^3$ as shown in Fig. 5.

Temperature

The connection between $F(\xi)$ and the temperature $T(\xi)$ involves the Schwinger mechanism (SM) for particle production. The Schwinger distribution for massless particles is expressed in terms of p_t^2 (Wong, 1994)

$$dn/dp_t^2 \sim e^{-\pi p_t^2/x^2} \quad (7)$$

where the average value of the string tension is $\langle x^2 \rangle$. The tension of the macroscopic cluster fluctuates around its mean value because the chromo-electric field is not constant. The origin of the string fluctuation is related to the stochastic picture of the QCD vacuum. Since the average value of the color field strength must vanish, it can not be constant but changes randomly from point to point (Bialas, 1999). Such fluctuations

lead to a Gaussian distribution of the string tension, which transforms SM into the thermal distribution (Bialas, 1999)

$$dn/dp_t^2 \sim e^{(-p_t \sqrt{\frac{2\pi}{\langle x^2 \rangle}})}; \quad \langle x^2 \rangle = \pi \langle p_t^2 \rangle_1 / F(\xi). \quad (8)$$

The temperature is expressed as (Scharenberg *et al.*, 2011; Dias and Pajares 2006).

$$T(\xi) = \sqrt{\frac{\langle p_t^2 \rangle_1}{2F(\xi)}} \quad (9)$$

Recently, it has been suggested that fast thermalization in heavy ion collisions can occur through the existence of an event horizon caused by a rapid de-acceleration of the colliding nuclei (Kharzeev *et al.*, 2007). The thermalization in this case is due to the Hawking-Unruh effect (Hawking, 1975; Unruh, 1976). The string percolation density parameter ξ which characterizes the percolation clusters measures the initial temperature of the system. Since this cluster covers most of the interaction area, this temperature becomes a global temperature determined by the string density. In this way at $\xi_c = 1.2$ the connectivity percolation transition at $T(\xi_c)$ models the thermal deconfinement transition. The temperature obtained using Eq.(9) was ~ 193.6 MeV for Au+Au collisions at $\sqrt{s_{NN}} = 200$ GeV in reasonable agreement with $T_i = 221 \pm 19^{stat} \pm 19^{sys}$ from the enhanced direct photon experiment measured by the PHENIX Collaboration (Adare *et al.*, 2010). For Pb+Pb collisions at $\sqrt{s_{NN}} = 2.76$ TeV the temperature is ~ 262.2 MeV for 0-5% centrality, which is expected to be ~ 35 % higher than the temperature from Au+Au collisions (Scharenberg *et al.*, 2011). A recent summary of the results from Pb+Pb collisions at the LHC has mentioned that the initial temperature increases at least by 30 % as compared to the top RHIC energy (Muller *et al.*, 2012).

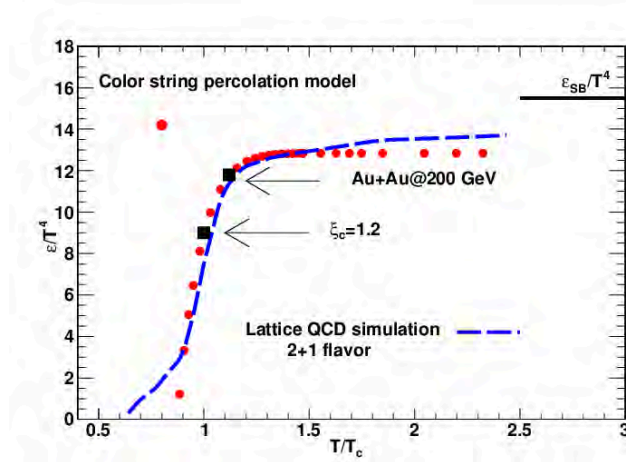


Fig. 6: ϵ/T^4 versus T/T_c from CSPM (red circles) and Lattice QCD (blue dash line) for 2+1 flavor and p4 action (Bazavov *et al.*, 2009)

One way to verify the validity of extrapolation from RHIC to LHC energy is to compare the energy density expressed as ε/T^4 with the available lattice QCD results. Fig. 6 shows a plot of ε/T^4 as a function of T/T_c . The lattice QCD results are from HotQCD Collaboration (Bazavov *et al.*, 2009). It is observed that at LHC energy the CSPM results are in excellent agreement with the lattice QCD results. The lattice and CSPM results are available for $T/T_c < 2$.

Shear Viscosity

The relativistic kinetic theory relation for the shear viscosity over entropy density ratio, η/s is given by (Hirano and Gyulassy, 2006)

$$\frac{\eta}{s} \simeq \frac{T\lambda_{mfp}}{5} \quad (10)$$

where T is the temperature and λ_{mfp} is the mean free path. $\lambda_{mfp} \sim \frac{1}{(n\sigma_{tr})}$ where n is the number density of an ideal gas of quarks and gluons and σ_{tr} the transport cross section. In CSPM the number density is given by the effective number of sources per unit volume $n = \frac{N_{sources}}{S_{NL}}$ L is the longitudinal extension of the source, $L = 1 \text{ fm}$ (Dias *et al.*, 2012). η/s is obtained from ξ and the temperature

$$\frac{\eta}{s} = \frac{TL}{5(1 - e^{-\xi})} \quad (11)$$

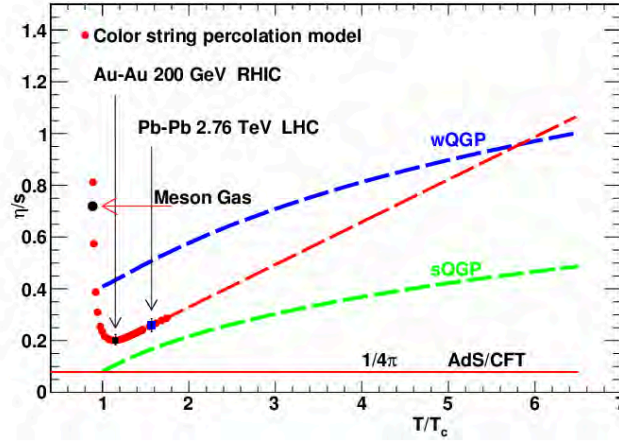


Fig. 7: η/s as a function of T/T_c . Au+Au at 200 GeV for 0-10% centrality is shown as solid black square. The estimated value for Pb+Pb at 2.76 TeV for 0-5% centrality is shown as a solid blue square. The red dotted line represents the extrapolation to higher temperatures from the CSPM. The hadron gas value for $\eta/s \sim 0.7$ is shown as solid black circle at $T/T_c \sim 0.88$ (Prakash *et al.*, 1993)

Fig. 7 shows a plot of η/s as a function of T/T_c . The η/s has been calculated both in the weakly (wQGP) and strongly (SQGP) coupled QCD plasma (Hirano and Gyulassy, 2006).

The theoretical estimate of η/s of wQGP and sQGP are shown in Fig.7 (Hirano and Gyulassy, 2006). The lower bound shown in Fig.7 is given by the AdS/CFT (Kovtun *et al.*, 2005). The results from Au+Au at 200 GeV and Pb+Pb at 2.76 TeV collisions show that the η/s value is 2.5 and 3.3 times the KSS bound (Kovtun *et al.*, 2005). It is seen that at the RHIC top energy η/s is close to the sQGP. Even at the LHC energy it follows the trend of the sQGP.

Equation of State

The equation of state(EOS) of QCD,(the pressure p , energy density ε , trace anomaly $\Delta = (\varepsilon - 3p)/T^4$, entropy $s = (\varepsilon + p)/T$, and the speed of sound $C_s^2 = dp/d\varepsilon$ as a function of the temperature) has been determined by several groups, however full result was still lacking. In this work we present CSPM results for Δ . The trace anomaly (Δ) is the expectation value of the trace of the energy-momentum tensor, $\langle \Theta_\mu^\mu \rangle = \varepsilon - 3P$, which measures the deviation from conformal behavior and thus identifies the interaction still present in the medium. We find that the reciprocal of η/s is in quantitative agreement with $(\varepsilon - 3P)/T^4$ over a wide range of temperatures as shown in Fig.8. The minimum in $\eta/s = 0.20$ at $T/T_c = 1.15$ determines the peak of the interaction measure ~ 5 in agreement with the recent values from HotQCD Collaboration (Petreczky, 2012). The Wuppertal-Budapest Collaborations results are also shown in Fig.8 (Borsanyi *et al.*, 2010). The maximum in Δ corresponds to the minimum in η/s . Both Δ and η/s describe the transition from a strongly coupled QGP to a weakly coupled QGP.

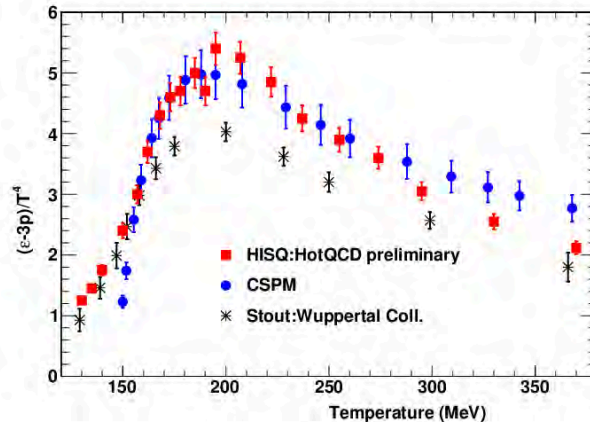


Fig. 8: The trace anomaly $\Delta = (\varepsilon - 3P)/T^4$ vs temperature (Borsanyi *et al.*, 2010)

Summary

A brief review of the color string percolation model is presented. It describes several observables in agreement with the experimental results. The thermodynamical quantities temperature and the equation of state

are obtained in agreement with the LQCD calculation. Thus the percolation approach within CSPM can be successfully used to describe the initial stages in high energy heavy ion collisions in the soft region.

Acknowledgement

This research was supported by the Office of Nuclear Physics within the U.S. Department of Energy Office of Science under Grant No. DE-FG02-88ER40412. The author thanks A Hirsch, C Pajares and R Scharenberg for fruitful discussions.

References

1. Aamodt K *et al.*, (2011) (ALICE Collaboration) Centrality dependence of charged particle multiplicity density at midrapidity in Pb-Pb collisions at $\sqrt{s_{NN}} = 2.76$ TeV, *Phys Rev Lett* **106** 032301
2. Abelev BI *et al.*, (2009) (STAR Collaboration) Systematic measurements of identified particle spectra in pp, d+Au and Au-Au collisions at the STAR detector, *Phys Rev* **C79** 34909
3. Adare A *et al.*, (PHENIX Collaboration) (2010) Enhanced production of direct photons in Au+Au collisions at $\sqrt{s_{NN}} = 200$ GeV and implications for the initial temperature, *Phys Rev Lett* **104** 132301
4. Bautista I, Milhano JG, Pajares C and Dias J de Deus (2012) Multiplicity in pp and AA collisions: the same power law from energy-momentum constraints in string production, *Phys Lett* **B715** 230
5. Bautista I, Dias J de Deus and Pajares C (2011) Elliptic flow at RHIC and LHC in the string percolation approach, arXiv:hep-ph/1102:3837
6. Bazavov A *et al.*, (2009) Equation of state and QCD transition at finite temperature, *Phys Rev* **D80** 014504
7. A Bialas (1999) Fluctuations of the string tension and transverse mass distribution, *Phys Lett* **B466** 301
8. Bjorken JD (1983) Highly relativistic nucleus-nucleus collisions: The central rapidity region, *Phys Rev* **D27** 140
9. Borsanyi S *et al.*, (Wuppertal-Budapest Collaboration) (2010) The QCD equation of state with dynamical quark, *JHEP* **11** 077
10. Braun MA and Pajares C (2000) Implications of color-string percolation on multiplicities, correlations, and the transverse momentum, *Eur Phys J* **C16** 349
11. Braun MA, Moral F del and Pajares C (2002) Percolation of strings and the relativistic energy data on multiplicity and transverse momentum distributions, *Phys Rev* **C65** 024907
12. Braun MA and Pajares C (2011) Elliptic flow from color strings, *Eur Phys J* **C71** 1558
13. Celik T, Karsch F and Satz H (1980) A Percolation approach to strongly interacting matter, *Phys Lett* **B97** 128
14. Dias J de Deus and Pajares C (2011) String percolation and Glasma, *Phys Lett* **B695** 455
15. Dias J de Deus, Hirsch AS, Pajares C, Scharenberg RP and Srivastava BK (2012) Clustering of color sources and the shear viscosity of the QGP in heavy ion collisions at RHIC and LHC energies, *Eur Phys J* **C72** 2123
16. Dias J de Deus and Pajares C (2006) Percolation of color sources and critical temperature, *Phys Lett* **B642** 455
17. Hawking SW (1975) Particle creation by black holes, *Commun Math Phys* **43** 199

18. Hirano T and Gyulassy M (2006) Perfect fluidity of the quark-gluon plasma core as seen through its dissipative hadronic corona, *Nucl Phys* **A769** 71
19. Isichenko MB (1992) Percolation, statistical topography, and transport in random media, *Rev Mod Phys* **64** 961
20. Kharzeev D, Levin E and Tuchin K (2007) Multiparticle production and thermalization in high-energy QCD, *Phys Rev* **C75** 044903
21. Kovtun PK, Son DT and Starinets AO (2005) Viscosity in strongly interacting quantum field theories from black hole physics, *Phys Rev Lett* **C94** 111601
22. McLerran L and Venugopalan R (1994) Computing quark and gluon distribution functions for very large nuclei, *Phys Rev* **D49** 2233
23. Muller B, Schukraft J and Wyslouch W (2012) First results from Pb+Pb collisions at the LHC, arXiv:hep-exp/1202.3233
24. Petreczky P (HotQCD Collaboration), Lattice 2012, Equation of state in 2+1 flavor QCD, Cairns, Australia, 24-30 June 2012
25. Prakash M *et al.*, (1993) Non-equilibrium properties of hadronic mixtures, *Phys Rep* **227** 321
26. Satz H (2012) Extreme States of Matter in Strong Interaction Physics, Lecture Notes in Physics 841
27. Scharenberg RP, Srivastava BK and Hirsch AS (2011) Percolation of color sources and the equation of state of QGP in central Au-Au collisions at $\sqrt{s_{NN}} = 200$ GeV, *Eur Phys J* **C71** 1510
28. Unruh WG (1976) Notes on black-hole evaporation, *Phys Rev* **D14** 870
29. Wong CY (1994) Introduction to high energy heavy ion collisions (World Scientific).